ELSEVIER

Available online at www.sciencedirect.com

SciVerse ScienceDirect

Energy Procedia 30 (2012) 1025 – 1034

Energy Procedia

SHC 2012

# Evaluation of turbulence models for airflow and heat transfer prediction in BIPV/T systems optimization

Siwei Li[a], Panagiota Karava[a*]

[a]School of Civil Engineering, Purdue University, 550 Stadium Mall Dr., West Lafayette 47907, USA

**Abstract**

Airflow patterns and convective heat transfer mechanisms in unglazed transpired solar collectors (UTCs) integrated with Photovoltaic-Thermal systems are crucial to their performance. Computational Fluid Dynamics (CFD) simulations can be a valuable tool for the design and analysis of these hybrid building-integrated solar energy systems while recent advances in CFD approaches and turbulence models provide a great potential for improving prediction accuracy. This study performs 3-dimensional steady Reynolds Averaged Navier-Stokes (RANS) CFD simulations and evaluates the performance of five turbulence closure models, potentially suitable for modeling UTCs in terms of accuracy and computing cost. These models include four two-equation models (Standard k-ε, Renormalization Group Methods k-ε, Realizable k-ε and Shear Stress Transport k-ω) and one Reynolds Stress Model. A flat UTC under free stream approaching flow conditions and a corrugated UTC subjected to a plane wall jet flow were considered. The predicted air velocity, air temperature, and turbulent kinetic energy were compared against experimental data from the literature and those obtained using a specially designed full-scale experimental set-up in a solar simulator. The results show that although the Reynolds Stress Model can provide more detailed flow features at an increased computational cost compared to other models, it does not necessarily result in better performance. Among the two-equation models, the Renormalization Group Methods k-ε has the best overall performance for both cases studied while the Standard k- ε and Shear Stress Transport k-ω models can also provide acceptable prediction accuracy. A BIPV/T system with two PV panel arrangements across a UTC under the same coverage was investigated using the CFD models developed in the present study. It was found that BIPV/T systems integrated with UTCs can result in electrical efficiency up to 1.2% higher, for the cases considered.



*Keywords*: Turbulence models; CFD; BIPV/T; UTC;

* Corresponding author. Tel.: +1-765-494-4573; fax: +1-765-494-0644.
*E-mail address*: pkarava@purdue.edu.


doi:10.1016/j.egypro.2012.11.115

## 1. Introduction

In unglazed transpired solar collectors (UTCs) a thin transpired metal sheet (flat or corrugated) is placed vertically alongside the building façade or horizontally on the roof to absorb solar radiation. The metal will heat up rapidly and transfer the heat to the air been forced to flow through the perforations and drawn into an air gap between the solar wall and the building [1]. The air gap is kept thin to ensure that all the air trapped in it maintains a high temperature. The hot air is drawn into ducts, either by a suction fan or by natural convection, to be used as free heat in HVAC systems (i.e. solar-assisted heat pumps, solar absorption cooling) or as direct supply air in dedicated outdoor air ventilation systems. In [2], it is stated that, although the concept is very simple, this UTC system is highly efficient, with thermal efficiency of 60% or more, as the heat lost to the ambient air can be recaptured by suction.

Furthermore, UTCs integrated with Photovoltaic panels, known as building-integrated Photovoltaic-Thermal (BIPV/T) systems, can generate electricity and heat, as shown in Fig 1(a). Recovering heat from the PV panel cools the panel thereby improving its electricity generation efficiency, resulting in 10% higher thermal efficiency than that of the standard UTC system and overall efficiencies that can be up to 70% [1, 3]. Despite its simple concept and cost effectiveness, the performance of this system is not well-understood, which is attributed to the complexity of the air flow, caused by the perforations and corrugation geometry, and its impact on convective heat transfer and consequently the overall thermal-electrical efficiency.

Airflow in this system is mainly driven by mechanical fans; however the strong solar radiation, that falls on the plate inducing thermal buoyancy effects, and the natural wind create complex airflow characteristics with impingement, separation, reattachment, etc. For the air velocity through the perforations, the Reynolds number is generally very low (namely $10^4$) while the Reynolds number of the wind flow over the plates is relatively high (namely $10^6$). Thus, the corresponding flow regime may span from laminar, transitional, to turbulent or combination of the above under transient conditions. This complexity of air flow makes experimental investigations difficult, expensive and time consuming.

Previous studies [4, 5, 6, and 7] mainly focused on analytical and experimental investigations due to the lack of advanced computational techniques. And the few numerical studies started by Kutscher [4] mainly conducted CFD simulations for laminar flow with the geometry limited to a pitch of a flat UTC or to one corrugation for a corrugated UTC under the assumption that UTCs are a combination of multiple pitches or corrugations with similar thermal performance. For example, Arulanandam et al. [8] simulated a quarter of pitch under no wind condition using a laminar Computational Fluid Dynamics (CFD) model and obtained a Nusselt (Nu) number correlation including the suction flow rate, perforation diameter, as well as the plate thickness, admittance and porosity. Gawlik et al. [7] studied the flow separation in a sinusoidal corrugation with a laminar CFD model and obtained a Nu number correlation based on corrugation amplitude and wavelength, suction velocity and wind speed. However, there is no previous study in the literature that has investigated the convective heat transfer process for the entire perforated plate subjected to realistic, turbulent approaching flow conditions, similar to those experienced by buildings, which are bluff bodies immersed in the atmospheric boundary layer.

With the rapid development of computer capacity and calculation speed, CFD techniques have become a powerful alternative for designing innovative solar energy systems. By solving the conservation equations of mass, momentum and energy, CFD modeling can provide quantitative answers, when properly validated, for various airflow and heat transfer parameters in this system. It offers a higher degree of flexibility and detail, i.e. it can distinguish convective heat transfer from radiation and can provide local convective heat transfer coefficients.

The goal of the present study is to develop models for the design and analysis of building-integrated photovoltaic/thermal systems combined with transpired air collectors, in which the objectives include (a) to test the accuracy of different turbulence closure models in evaluating the complex convective heat transfer process on both flat and corrugated UTCs using CFD simulations; and (b) to compare and analyze the cooling capability and thermal efficiency of different PV panel arrangements mounted on identical corrugated UTC's under turbulent approaching flow conditions, as shown in Fig 1(b).

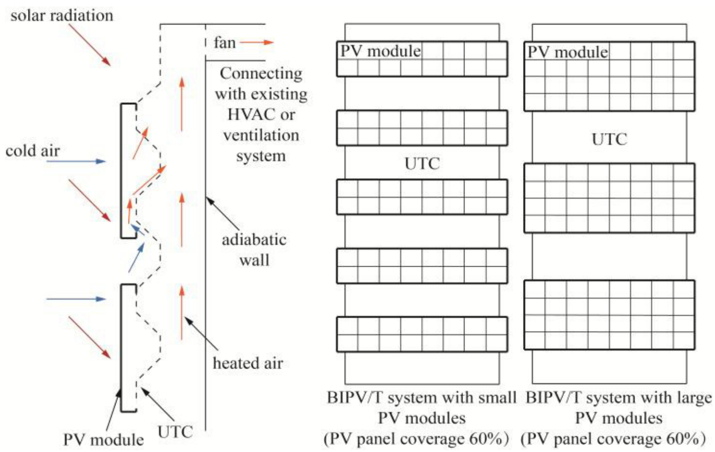


Fig. 1. (a) Schematic sketch of BIPV/T system integrated with corrugated UTCs; (b) different PV panel arrangement across identical UTCs

In [1], experiments have been conducted to compare the thermal energy recovery of two identical UTC systems integrated with two types of PV modules, similar as in Fig 1(b). The results indicated that a UTC system with smaller modules can recover 30% more thermal energy than the system with larger modules. The present study will simulate these two scenarios with a CFD model to provide insights in convective heat transfer process for design analysis and optimization.

## 2. Methodology

The commercial CFD software, ANSYS (version 13.0) was used to conduct all the 3-D steady numerical simulations discussed in this paper and GAMBIT 2.4.6 was used for all geometry models. Five RANS models (Standard k-ε, Renormalization Group Methods k-ε, Realizable k-ε, Shear Stress Transport k-ω with low Reynolds number correction and the Reynolds Stress Model) have been evaluated. A second order upwind spatial discretization scheme was adopted for all the variables except pressure, which is using PRESTO!. The discretization of pressure is based on a staggered scheme. The SIMPLE algorithm was used to couple the pressure and momentum equations. If the sum of absolute normalized residuals for all the cells in the flow domain became less than $10^{-6}$ for energy, $10^{-5}$ for velocity components and $10^{-4}$ for other variables, the solution was considered converged. Grid independence for each case was checked using three different grids to ensure that grid resolution would not have a notable impact on the results. In all simulations enhanced wall treatment was applied to maintain a y* value around 1.

### *2.1. Flat UTC model*

Fig 2(a) shows the computational domain and geometry model for the flat UTC. In the region above the plate, the left side of the domain was defined as the velocity-inlet with a specified approaching flow velocity and the right side of the domain was defined as the pressure-outlet with zero gauge pressure. The plate was set to be a wall with thickness of 0.00086m and the perforations on the plate were set to be ‘interior’. The bottom of the cavity was defined as velocity-outlet with a specified suction velocity. The left and right side of the cavity were defined as adiabatic walls. A symmetry boundary condition was used for all other faces, which means zero velocity and temperature gradient. The upper domain is 0.3m height, which is sufficient for the boundary layer growth.

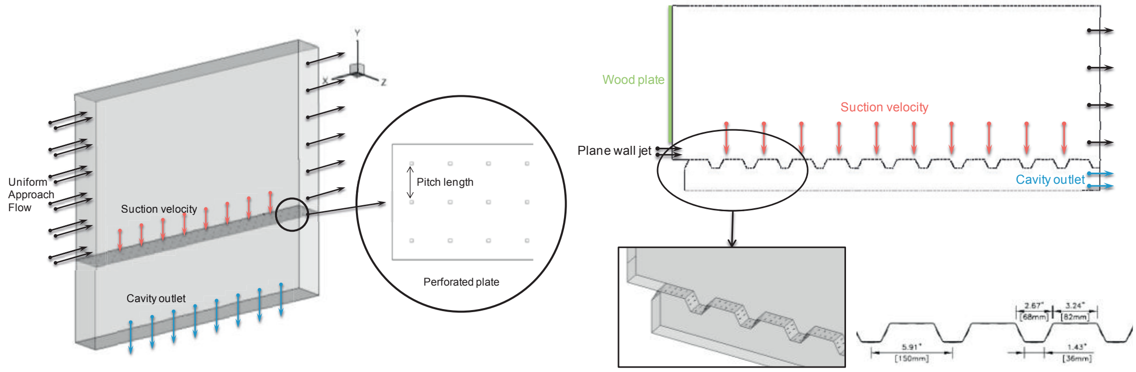


Fig. 2. (a) Computational domain for flat UTC; (b) Dimensions and computational domain for corrugated UTC

A horizontally placed, perforated plate with an area of 0.6m x 0.6m and a cavity with 0.15m height were considered. The plate has pitch length of 0.01689 m and perforation diameter of 0.00159 m. Considering the small size of the perforations, their shape was assumed to be square, instead of the circular shape used in the experimental set-up [6], for model simplicity. The simulated solar radiation in the experiments was around 600W/m$^2$, the ambient air temperature was 298K, and the turbulence intensity of incoming flow was 0.8%, which is considered to be uniform. These values were used as inputs in the CFD model.

## *2.2. Corrugated UTC model*

An experimental set-up was designed for testing a 1.73m x 1.58m transpired corrugated collector in a facility equipped with a solar simulator under uniform simulated solar radiation of 1029W/m$^2$. The solar simulator consists of a set of eight lamps (dimmable) that can accurately reproduce the solar spectrum and irradiance levels. A hotwire anemometer was used for measuring the three components of the velocity, turbulence intensity and Reynolds stresses. Because the exit size of the blower is only 5.5cm, the entire corrugated plate was subjected to a plane wall jet rather than a free stream flow. A wood plate with a height of 0.55m was placed above the fan exit to reduce the entrainment of ambient air and obtain a pure wall jet without co-flow. Parameters which have been measured for the model validation are the ambient air temperature, the air temperature in the cavity and the exit, the surface temperature along the plate, the simulated wind speed and turbulent kinetic energy, the suction flow rate, and the uniformity of the incident simulated solar radiation.

Fig 2(b) shows the dimensions and the computational domain for the corrugated UTC. All dimensions and inputs used in the CFD model are the same with those in the experiments. The plate thickness is 0.5842mm and the cavity exit height is 0.095m. Also considering the small size of the perforations, their shape was assumed to be rectangular, instead of the triangular shape used in the experiments, for model simplicity. The simulated normal solar radiation in the experiments was around 1023W/m$^2$, the ambient air temperature was 297K, and the turbulence intensity of incoming flow was around 6%.

### *2.3. Corrugated UTC integrated with PV panel model*

In this configuration, the geometry of the UTC is the same as in Section 2.2. The large PV modules cover 1.06m$^2$ of UTC area while the coverage area is 1.05m$^2$ in the case with small PV modules, as shown in Fig 3. Since the purpose of this study is to investigate how the presence of PV modules would affect the convective heat transfer process in the system, the impact of the PV material itself and especially its thermal capacitance were not considered. Therefore, the PV modules are modeled as simple ordinary plates, rather than taking all the material layers into consideration. The PV module considered here is polycrystalline silicon for its high electrical efficiency and ease of installation (mounting) on the exterior side of UTCs [1].

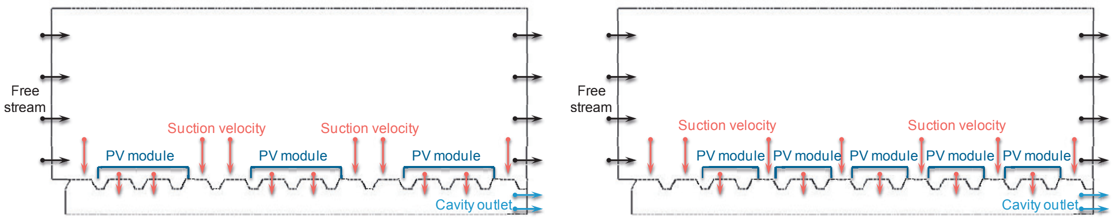


Fig. 3. Schematic of PV module arrangement used in the simulation, both with coverage around 60% of UTC area: (a) large modules; (b) small modules

In this case, a 3m/s free stream velocity was assumed with normal solar radiation at the surface of 1000W/m$^2$ and suction velocity varying between 0.015m/s and 0.065m/s, as typically found in practical applications. The turbulence intensity of incoming flow was set to be 0.1% in order to obtain uniform approaching flow conditions and reduce the irrelevant interference, such as unexpected entrainment or turbulence caused by the irregular approaching flow working together with the complex geometry. Also, the simulated plate was horizontally placed to eliminate the effect of vertical stratification.

## 3. Results and discussion

### *3.1. Flat UTC model validation*

The suction velocity simulated in the tested cases for flat UTC model varies from 0.045m/s to 0.074m/s and a wind speed of 1m/s or no-wind conditions have been adopted according to the experimental data. The average plate surface temperature and cavity outlet temperature computed using different RANS models are compared with the experimental data and the results are shown in Fig 4 (a, b). The RSM was only used for isothermal conditions due to the difficult convergence process of this model for non-isothermal cases.

For the plate surface temperature, the agreement between CFD results and experimental data is satisfactory with the error within 2K. The Standard k-ε and the RNG k-ε model give similar results with the Realizable k-ε model but are more stable in terms of convergence and more consistent. The performance of the SST k-ω model is different than all the k-ε models with the results showing that the surface temperature is slightly overestimated, but still the modeling error is considered acceptable.

For the cavity outlet temperature, all models provided identical results. Thus, based on this comparison, all the RANS models tested here, except the Realizable k-ε model, can provide sufficiently accurate results for thermal modeling in flat UTC models.

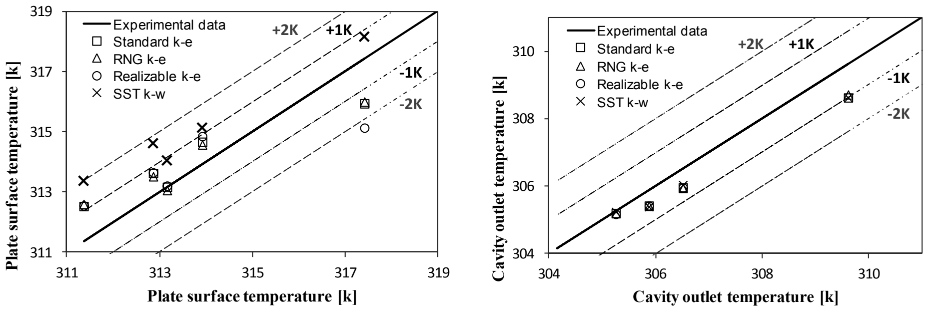


Fig. 4. Comparison between CFD and experimental results for the flat UTC model: (a) average plate surface temperature; (b) cavity outlet temperature

### *3.2. Corrugated UTC model validation*

For the corrugated plate under plane wall jet, both isothermal and non-isothermal conditions were considered in the simulation. In the isothermal case, the core region speed at the jet exit is 5.85m/s with turbulence intensity of 5.6% and the suction mass flow rate is 392kg/hr, corresponding to a suction velocity of 0.033m/s. The vertical velocity and turbulence kinetic energy profile at six crests computed with all the RANS models have been compared with experimental results, as shown in Fig 5 and Fig 6, in which x is the stream-wise distance and b is the jet exit height.

In Fig 5, the error bar stands for the measurement uncertainty which is 10% after calibration. It can be seen that the agreement between the CFD simulation results and experimental data is very good in the near wall region (within 0.03m), which affects the heat transfer process most, especially for the RNG k-ε model, which can provide accurate prediction with the error within the 10% measurement uncertainty range. This is due to the fact that the RNG model has an additional term in epsilon equation and a swirl modification which improves the accuracy for rapidly strained flow and swirling flows, i.e. the suction flow through the perforations and the separation flow over the corrugations. Also it provides an analytical formula for turbulent Pr number rather than a constant value used in other turbulence models. At larger height all models overestimate the decay of the jet in the vertical direction; however, the prediction is still within the 20% modeling error range, except in the case with the Realizable k-ε model.

The general shapes of turbulent kinetic energy profiles predicted by the CFD simulations match with the experimental data, but differences in the specific values exist. The measurement uncertainty for turbulent kinetic energy is 14% after calibration, as shown with the error bars in Fig 6. Among all the RANS models tested, none of the turbulence models can provide accurate prediction within the measurement uncertainty, but the prediction from RNG k-ε model is almost within the 20% modeling error range. The results from the Standard k-ε model and SST k-ω model bias more than the RNG k-ε model and are within the 30% modeling error. Along the stream-wise direction, the prediction of RSM differed greatly from the experimental data, but it got better after x/b=24, within the 30% modeling error. Therefore, although RSM can provide more detailed flow information, i.e. Reynolds stresses, at a much higher computational cost and effort compared to the two-equation models, it does not result in more accurate predictions for the cases considered here.

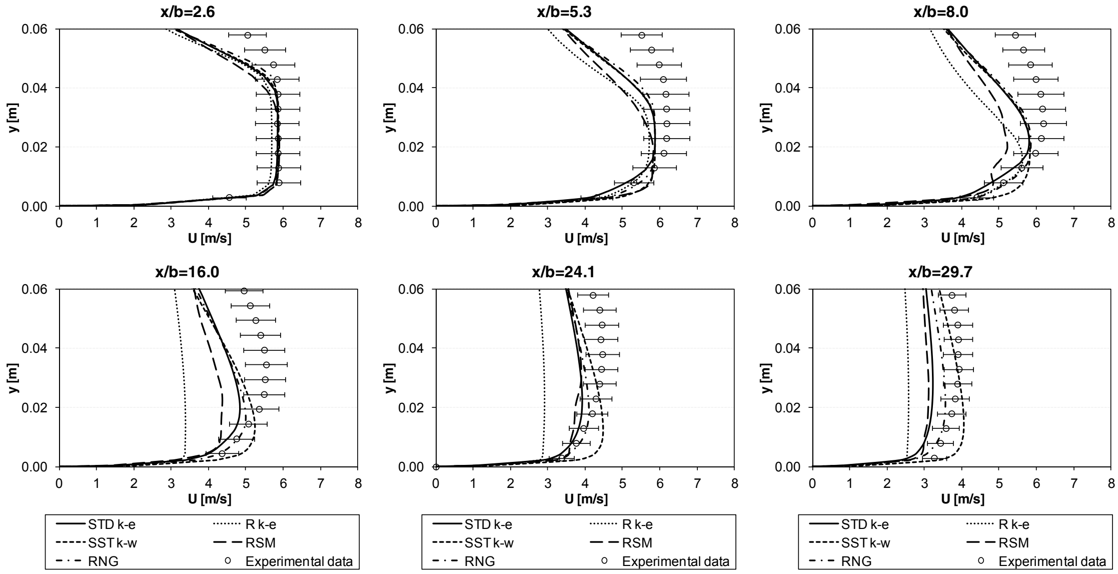


Fig. 5. Velocity profiles in the stream-wise direction for the corrugated UTC model - comparison between CFD and experimental results for isothermal conditions

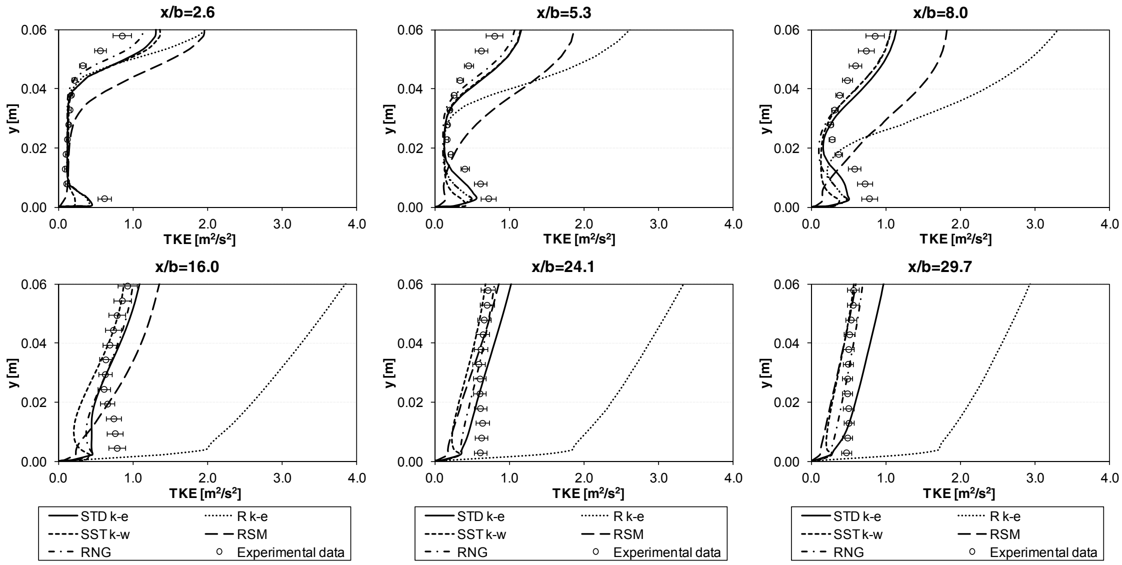


Fig. 6. Turbulent kinetic energy profiles in the stream-wise direction for the corrugated UTC model - comparison between CFD and experimental results for isothermal conditions

In the non-isothermal case, the core region speed at the jet exit is 8.59m/s with a turbulence intensity of 5.8% and the suction mass flow rate is 392kg/hr, corresponding to a suction velocity of 0.033m/s. The surface plate temperature at each crest ($3^{rd}$ -$10^{th}$) and the cavity outlet air temperature were computed and compared with the experiments data as shown in Fig 7. Based on the investigations for the isothermal case, the Realizable k-ε model was deemed to be inaccurate and it was not considered in this case. Generally, the Realizable k-ε model is expected to give more accurate prediction for the spreading rate of both planar and round jets for its different formula of turbulent viscosity and dissipation rate; however, this feature does not provide superior performance for suction flows together with irregular corrugations. From Fig 7, it can be concluded that all the three RANS models tested performed well, with the error within 2K, among which the RNG k-ε model shows the best performance with the error within 1K.

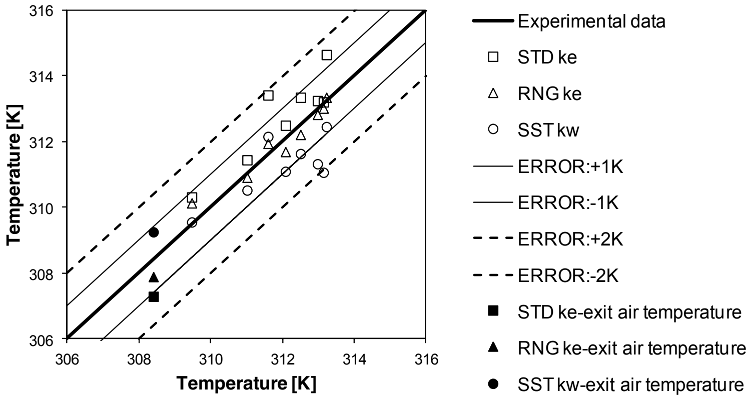


Fig. 7. Crest surface temperature and cavity outlet air temperature for the corrugated UTC model - comparison between CFD and experimental results for non-isothermal conditions

In summary, the best match between the experimental data, reported in [6] and collected from the new test facility, and the CFD results in terms of plate surface and exit air temperature, vertical velocity and turbulent kinetic energy profiles was obtained with the RNG k-ε model. Therefore, the following analysis of the BIPV/T system was conducted using the RNG k-ε model.

### *3.3. Optimization analysis for a BIPV/T system with two types of PV panel arrangements across a UTC*

The optimal integration of PV panels with UTCs is seeking the maximum electricity generation and heat recovery for a certain PV panel coverage. In CFD simulations, it is impossible to calculate the electricity produced by the PV modules, so an alternative index of the PV module efficiency would be the cooling capability of the UTC system, which can be estimated based on the surface temperature of PV modules using the following typical linear expression [9]:

$$\eta_T = \eta_{Tref}[1 - \beta_{ref}(T - T_{ref})] \qquad (1)$$

where $\eta_T$ is the PV electrical efficiency at temperature T; $\eta_{Tref}$ equals to 0.15 and is the PV electrical efficiency at 298K reference temperature ($T_{ref}$) and solar radiation flux of 1000W/m$^2$; $\beta_{ref}$ is the temperature coefficient equal to 0.0041K$^{-1}$. From Fig 8 (a) it can be seen that with the increase of suction flow rate the surface temperature of PV modules can decrease from 350K to 330K, which corresponds to an efficiency increment of 1.2%. Also, the average surface temperature of each PV module will increase in the stream-wise direction, but this variation will become zero when the suction velocity keeps rising up. This indicates that overheating of down-stream PV modules can be avoided with higher suction flow rates by maintaining the convective heat transfer rate along the stream-wise direction. It is also observed that the surface temperature of large PV modules is 4-5K higher than that of small PV modules, which corresponds to 0.3% lower PV efficiency.

Also as shown in Fig 8 (b) almost the same thermal efficiency is obtained for the two types of PV modules, with the small modules resulting in about 3% higher values. Thus, the thermal efficiency augmentation with the smaller modules is very limited in the present study, compared to the 30% increase reported in [1]. It is likely attributed to other factors influencing the test results in [1], which are not related to the geometry, such as the material properties of the PV module, the absorptance, etc.

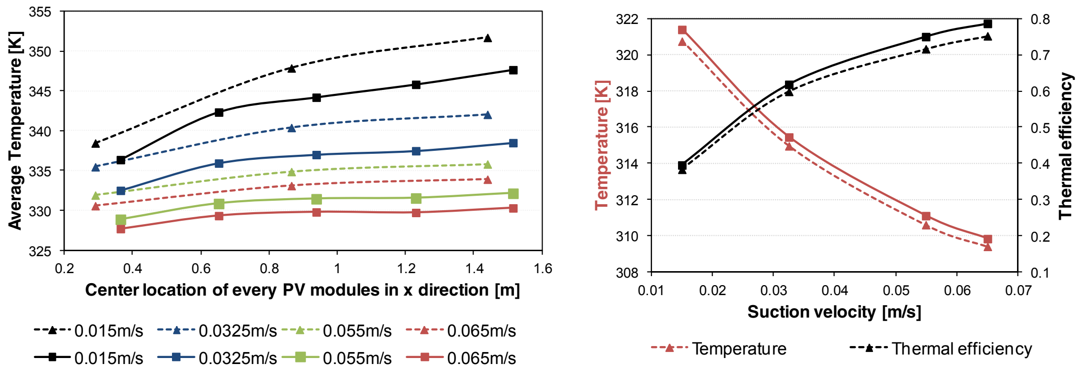


Fig. 8. Comparison between the two PV panel arrangements in terms of (a) surface temperature of PV modules at different suction velocities; (b) exit air temperature and thermal efficiency; (here dash lines correspond to large modules and solid lines to small modules)

## 4. Conclusions

Based on the results presented in this study, it can be concluded that CFD simulations are a reliable, valuable and convenient tool for design, analysis and optimization of BIPV/T systems integrated with UTC plates. The performance of five RANS turbulence models have been tested for two cases: a flat UTC under free stream approaching flow and a corrugated UTC subjected to a plane wall jet flow. By comparing the surface and air temperature, vertical velocity and turbulent kinetic energy profiles, the results show that the RNG k-ε model has the best overall performance for both cases studied. The Standard k-ε model and the SST k-ω model did not perform as well as the RNG k-ε model, but they can still provide acceptable predictions. Although the RSM requires more computing cost and effort, it was selected in this study as it can provide detailed flow information. However, it did not provide better modeling accuracy than the other models. The results from the Realizable k-ε model differed a lot from those obtained using the other models and the experimental data, which indicates that it is not suitable for modeling the UTC system.

The analysis for a BIPV/T system with two types of PV panel arrangement revealed that under the wind speed of 3m/s, the system integrated with a corrugated UTC can provide a higher electrical efficiency (up to 1.2%) which will increase for higher suction velocity. The small PV modules can provide slightly higher overall efficiency compared to a system with larger PV modules covering the same area. Further research will be focused on the optimal system performance under various approaching flow conditions and suction velocities, with different PV cell and module technology, coverage area and UTC type.

## Acknowledgements

The authors are grateful to Professor Andreas Athienitis for providing access to the solar simulator at Concordia University. This work would not have been possible without the help from Professor Eric Savory, Dr. Will Lin (University of Western Ontario) and Mr. James Bambara (Concordia University).

## References

[1] Athienitis AK, Bambara J, O'Neil B, Faille J. A Prototype Photovoltaic/thermal System Integrated with Transpired Collector. *Solar Energy* 2011; **85**:139-153.

[2] Kutscher CF, Christensen C, Barker G. Unglazed transpired solar collectors: heat loss theory. *ASME J. Solar Eng.* 1993; **115**: 182-188.

[3] Bambara J, Athienitis AK, Karava P. Performance Evaluation of a Building-Integrated Photovoltaic/Thermal System. *Proceedings of International High Performance Buildings Conference at Purdue* 2012.

[4] Kutscher CF. An investigation of heat transfer for air flow through low porosity perforated plates. *Ph.D. Thesis*, Department of Mechanical Engineering, University of Colorado at Boulder, Colorado, USA; 1992.

[5] Golneshan AA. Forced Convection Heat Transfer from Low Porosity Slotted Transpired Plates. *Ph.D. Thesis*, Department of Mechanical Engineering, University of Waterloo, Waterloo, Canada; 1994.

[6] Van Decker GWE, Hollands KGT, Brunger AP. Heat-exchange relations for unglazed transpired solar collectors with circular holes on a square or triangular pitch, *Solar Energy* 2001; **71**: 33-45.

[7] Gawlik KM. A numerical and experimental investigation of heat transfer issues in the practical utilization of unglazed, transpired solar air heaters. *Ph.D. Thesis*, Department of Civil, Environmental, and Architectural Engineering, University of Colorado, Colorado, USA; 1993.

[8] Arulanandam SJ, Hollands KGT, Brundrett E. A CFD heat transfer analysis of the transpired solar collector under no-wind condition. *Solar Energy* 2000; **67**: 93–100.

[9] Skoplaki E, Palyvos JA. On the temperature dependence of photovoltaic module electrical performance: A review of efficiency/power correlations. *Solar Energy* 2009; **83**: 614-24.